J Mater Sci (2008) 43:4192–4197
DOI 10.1007/s10853-008-2599-9

Influence of silver doping on the physical properties of Mg ferrites

N. Okasha

Received: 16 May 2007 / Accepted: 17 March 2008 / Published online: 10 April 2008

Abstract The physical properties of silver substituted magnesium ferrite $MgAg_xFe_{2-x}O_4$ ($0.0 \leq x \leq 1$) have been studied as a function of silver ion concentration. The samples were prepared using the flash combustion technique. The effect of Ag content on microstructure and magnetic properties has been studied. X-ray diffraction (XRD) analysis reveals the spinel structure besides metallic silver particle at all concentrations. The decrease in the lattice constant with increasing Ag up to the critical concentration ($x = 0.2$) was discussed. The close agreement of the theoretical and experimental lattice constant ratio from XRD pattern supports the occupancy of silver on the tetrahedral sites. The morphological features were studied using scanning electron microscope. The magnetic susceptibility, Curie temperature (T_C), and effective magnetic moment (μ_{eff}) were decreased with compositional parameter. The DC electrical conductivity of the investigated samples was measured and the results indicated the increase in conductivity with increasing Ag content from 5.6×10^4 at $x = 0$ to $12.6 \times 10^4 \Omega^{-1}$ cm^{-1} at $x = 1$. The transition from the ferrimagnetic to paramagnetic state is accompanied by an increase in the thermo EMF. Ag–Mg ferrite shows p-type conductivity at all concentrations of Ag particles where the creation of lattice vacancies is due to presence of Ag^+ ions gives rise to the p-type conductivity.

N. Okasha (✉)
Physics Department, Girls College, Ain Shams University, Cairo, Egypt
e-mail: naokmo@yahoo.com

Introduction

In the past few years, mixed ferrites have attracted much attention because of their vast applications, ranging from microwave to radio frequencies such as microwave devices, computer memories, and magnetic recording [1–3]. They are distinguished by their resistivity and low eddy current losses. A modification of both structure and transport properties are obtained by introducing a relatively small amount of rare earth elements [4]. These properties are mainly depending on the amount of constituents and preparation conditions.

The ferrite $MgFe_2O_4$ is a well-known spinel (space group *Fd-3m*) with a cation distribution that can be represented as $(Mg_{1-t}\ Fe_t)_{8A}\ [Mg_t\ Fe_{2-t}]_{16B}$, where t depends on the thermal treatment [5] and it has a ferrimagnetic structure with Curie temperature depending on the cation distribution. The crystal structure of silver belongs to the space group *Fm-3m* with cubic close packed which consist of a deformed face-centered cubic metal atom arrangement with equal proportions of linear coordinated Ag (I) and approximately square-planar coordinated Ag (II) [6–8].

Early X-ray powder diffraction data on samples which were synthesized by oxidation of Ag by Ozone [9] were built up by a usual combination of Ag (I) and Ag (II), O_2^{2-}, and O^{2-} ions [10]. The presence of high loadings of metallic Ag in any ferrite seems to be very important since it significantly increases the thermal and electrical conductivity as well as improving the mechanical strength of the fabricated composites. Furthermore, the addition of Ag acts as a flux in reducing porosity and improving density as well as decreasing the sintering temperature. All these effects are distinctly influenced by the changes in microstructure and grain links in the sample [11]. In literature there is no report about the preparation, physical properties, or characterization of substituted Ag ferrites.

Almost all silver compounds with predominantly ionic bonding properties are light sensitive and in many cases also thermally sensitive. Though there have been a few investigations on silver such as Ag–Mn [12] and Ag–Bi [13], its various properties such as thermal decomposition kinetics, structure, magnetic measurements [7], and resonance Raman work were studied by many authors [14–17].

The aim of the present work is to study the effect of Ag substitution on the behavior of the physical properties of Mg ferrites where the results suggested that, Ag metal ions can be used as an electrode material as applicable.

Experimental techniques

The cubic form of silver magnesium ferrite with the representative formula $MgAg_xFe_{2-x}O_4$ ($0.0 \leq x \leq 1$) was prepared by flash combustion technique [18] where the constituent precursor salt solutions of the desired compositions are mixed thoroughly to ensure the molecular level of mixing and heated to form oxides. The raw materials used in this preparation were magnesium nitrate [Mg $(NO_3)_2 \cdot 6H_2O$], silver nitrate [Ag (NO_3)], ferric nitrate [Fe $(NO_3)_3 \cdot 9H_2O$], and urea. According to the required stoichiometric proportion, the pure nitrates were mixed well in an agate mortar for few minutes. Urea was added to the mixture (as fuel) and again mixed thoroughly. The mixture was transformed to quartz crucible and introduced into an electric furnace (Lenton furnace 16/5 UAF England) kept at 500 °C. At this temperature, the mixture reacted leading to combustion and the reaction was complete in 30 min. A foamy and highly porous precursor mass was obtained. The product was collected and then powdered for further processing. The ferrite precursor powder was calcined at 900 °C for 1.5 h then pressed into pellets using uniaxial press using pressure of 1.9×10^8 N/m^2 and finally sintered at 1,250 °C for 2 h. For sintered sample phase characterization, X-ray diffraction (XRD) pattern was performed using diffractometer (*Proker D_8 USA*) with CuK_α radiation ($\lambda = 1.5418$ Å). The bulk density was determined by using Archimedes method. The microstructure of the sintered composites was analyzed by field emission scanning electron microscope (SEM) (*JEM-100S*). The dc molar magnetic susceptibility of homogeneous solid solution was measured using Faraday's method at different magnetic field intensity ranging 800–2,160 Oe and temperature between 300 and 600 K where the sample was inserted in the point of maximum gradient. The measurements were performed over a temperature range where a paramagnetic behavior was observed in all the samples. The dc electrical resistivity (ρ_{dc}) was measured from room temperature up to 600 °C using the two-probe method. The thermoelectric power measurements were carried out in the same temperature range by maintaining a temperature difference of 10 °C between hot and cold junctions to determine the type of conductivity.

Results and discussion

Structural properties

The effect of the silver ions on the structure of the samples $MgAg_xFe_{2-x}O_4$ ($0.0 \leq x \leq 1$) was shown as a typical chart in Fig. 1. The data show that, in the whole composition, samples possess metallic silver together with the cubic spinel phase. The relative intensities of silver peaks increase with increasing silver content. Despite the fact that the sintering process was conducted in air, no silver oxide is found in Mg–Ag ferrites, where the thermodynamical study [19] has suggested that, the metallic silver is more stable than silver oxide at a temperature higher than 189.8 °C. The calculated value of the lattice constant decreases with increasing (x) up to the critical concentration ($x = 0.2$) and then increases slightly, to give nearly stable values as in Fig. 2 and Tables 1 and 2. This may be logically attributed to the difference between the ionic radius of Fe^{3+} (0.64 Å) and Ag^{1+} (1.26 Å) ions. When Ag^{1+} ions increase at the expense of Fe^{3+} ions, the volume of the unit cell be decreased well. Moreover, the observed slight increase in unit cell constant (a) with increasing (x) can easily be understood from the predicted

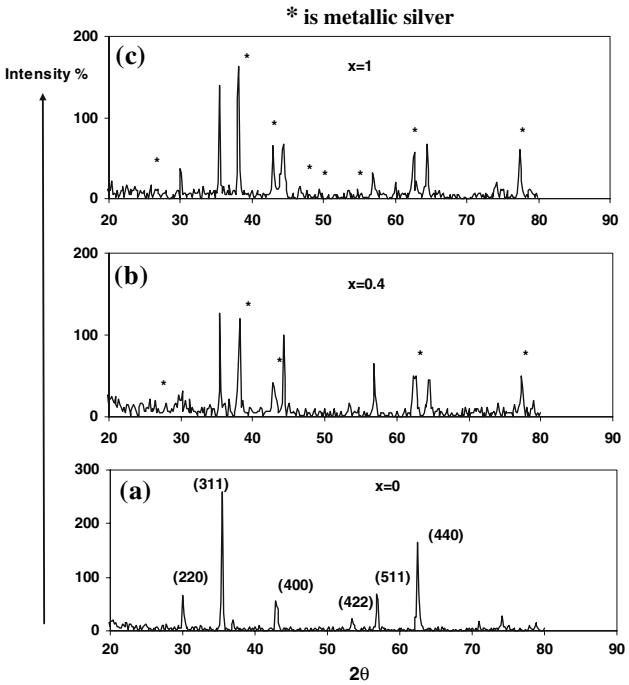

Fig. 1 XRD pattern for $MgAg_xFe_{2-x}O_4$; $0 \leq x \leq 1$

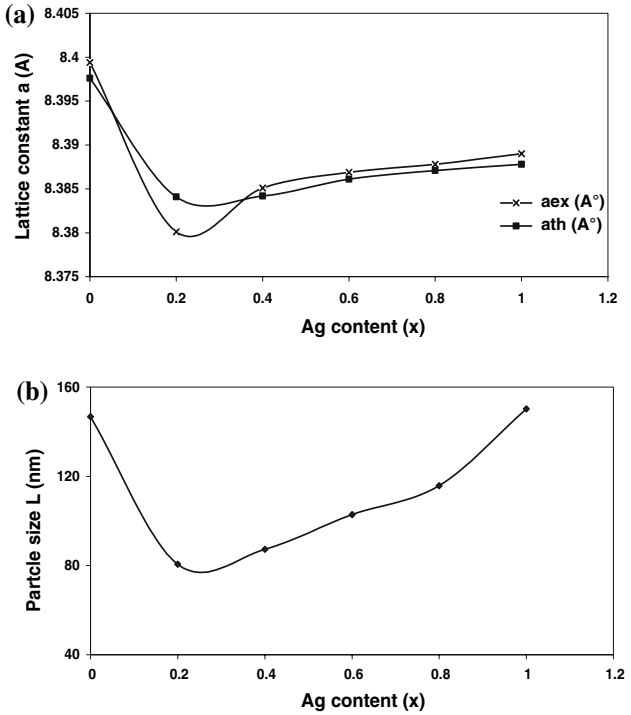

Fig. 2 (**a**) Comparison between the experimental (a_{ex}) and theoretical lattice constant (a_{th}) as a function of Ag content (x). (**b**) The variation of crystal size (L) as a function of Ag content (x)

Table 1 The values of experimental lattice constant (a_{ex}), theoretical lattice constant (a_{th}), bulk density (D), X-ray density (D_x) porosity ($P\%$), and the grain size (L)

x	a_{ex} (Å)	a_{th} (Å)	D_x (g/cm^3)	D (g/cm^3)	$P\%$	Particle size L (nm)
0	8.3994	8.3976	4.483	4.327	3.63	146.8
0.2	8.3801	8.3841	4.749	4.681	1.42	80.6
0.4	8.3851	8.3842	4.953	4.862	1.83	87.3
0.6	8.3869	8.3861	5.188	5.077	2.25	102.9
0.8	8.3878	8.3871	5.426	5.315	2.15	115.8
1	8.389	8.3878	5.658	5.587	1.32	150.2

Table 2 The values of effective magnetic moment m_{eff}, Curie temperature T_c, and exchange interaction J for the system $MgAg_xFe_{2-x}O_4$ $0 \leq x \leq 1$

x	μ_{eff}				T_c (k)	J (eV/K)
	833 Oe	1,280 Oe	1,733 Oe	2,160 Oe		
0	5.98	5.27	4.9	4.08	593	14.56
0.2	5.83	5.04	4.7	3.92	553	13.81
0.4	4.79	4.61	4.49	3.94	553	13.81
0.6	4.38	4.18	3.98	3.62	573	14.18
0.8	3.9	3.73	3.71	3.53	583	14.3
1	3.43	3.32	3.26	2.95	583	14.3

variation of the cation distribution. Mg^{2+} is a highly diffusible ion and is very sensitive to heat treatment with regard to its site occupancy in the spinel lattice. $MgFe_2O_4$ has been reported by Verwey and Heilman [20] to have a random cation distribution where a fraction of the Mg^{2+} ions displace an equivalent number of Fe^{3+} from octahedral sites (B) where Mg^{2+} ions have a strong preference to occupy B sites and partially occupy A sites [21]. Due to the larger ionic radius of Ag^{1+} ions, they cannot diffuse in the spinel matrix and form small aggregates of secondary phase on the grain boundaries. As a result, some of Fe^{3+} ions change their valence into Fe^{2+} ions to keep charge neutralization. By increasing Ag^{1+} ion content, some of Fe^{2+}ions formed on the B sites migrate to the A sites, which in turns leads to an increase in the lattice parameter with Ag content. After $x = 0.4$, the Ag^{1+} ion phase becomes predominant and makes the spinel lattice nearly of stable volume.

The values of the lattice constant both experimental and theoretical enhance out expectation as in Fig. 2a. It is noticed that there is a good agreement between the lattice constant of the prepared sample (8.3994 Å) and that reported in the JCPDS cards (No. 36.0398) (8.3879 Å) for the sample with $x = 0$ ($MgFe_2O_4$). The theoretical lattice constant a_{th} of the investigated samples was calculated from the equation [22]:

$$a_{th} = \frac{8}{3\sqrt{3}}[(r_A + R_0) + \sqrt{3}(r_B + R_0)],$$

where R_0 is the radius of oxygen ion (1.32 Å), r_A and r_B are the ionic radii of the tetrahedral and octahedral sites, respectively. Using the experimental values of lattice constant, the X-ray density (D_x) was calculated using the equation: $D_x = 8\ M/Na^3$ where M is the molecular weight, N is Avogadro's number. The values of (D_x), bulk density (D), and porosity $P\%$ were calculated and listed in Table 1. The data reveal that, the density increases with increasing Ag content according to the increase in atomic weight which is (107.870) for Ag and (55.847) for Fe. Also, the porosity was calculated from the relation: $P\% = (1 - D/D_x) \times 100$. The results clarify that the porosity has the opposite trend of the density with increasing Ag content. This trend may be due to the creation of more cation vacancies with the reduction in oxygen vacancies which play a predominant role in acceleration densification, i.e., the decrease in oxygen ion diffusion would retard the densification.

The particle size (L) was calculated from the full width at half maximum of (311) diffraction peak and plotted versus Ag content (x) (Fig. 2b). The data show that, the grain size increases with increasing Ag content after

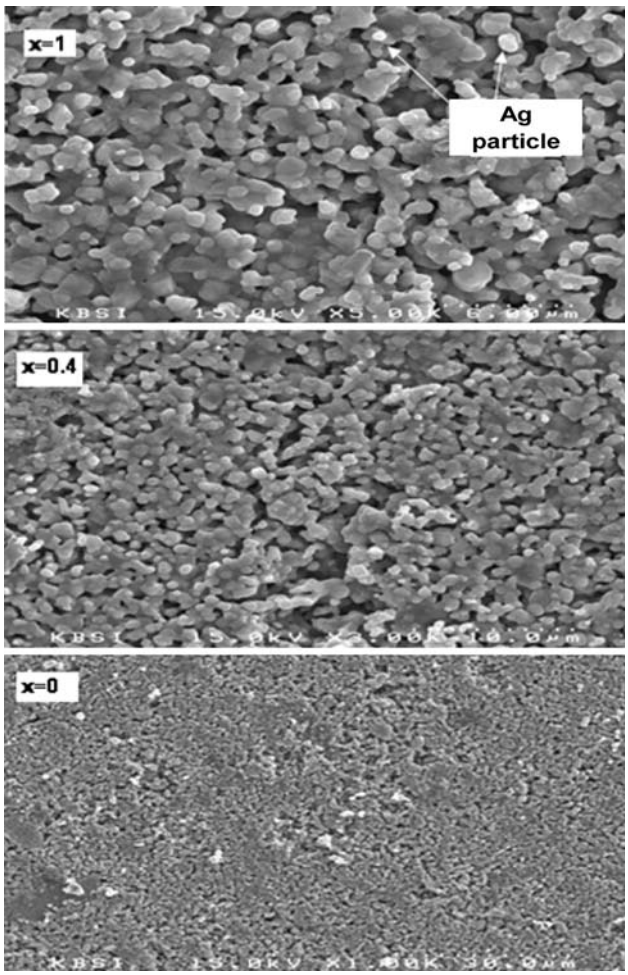

Fig. 3 The image of micrograph SEM of the $MgAg_xFe_{2-x}O_4$; $0 \leq x \leq 1$

$x = 0.2$. This result was explained by the migration of Fe^{3+} ions from B sites to A sites as mentioned before.

To confirm the homogeneity of the sample, SEM was carried out. Figure 3 shows typical SEM for the investigated samples, where abnormal grain growth occurs and trapped pores remain inside grains regardless of the amount of Ag particles. This appeared in all concentrations and these agree well with XRD patterns. In other words, small Ag particles are homogeneously dispersed around grain boundaries but relatively large Ag particles are agglomerated. From these observations, it could be deduced that Ag^{1+} ions form a liquid phase during the sintering process, which is in accordance with the previously reported data [20] about the role of sintering additives in Ag–Mg ferrite. Thus, the formation of a liquid phase during sintering decreases the sintering temperature of the investigated ferrite by enhancing the diffusion rate [23]. Accordingly, a careful controll of Ag composition and sintering temperature is required for optimizing the microstructure.

Magnetic properties

The magnetic properties of spinel ferrites are determined largely by the distribution of the cations on A and B sites. The cation distribution can be suitably modified by addition of impurity cations or by controlling the preparation conditions, particularly heat treatment. Figure 4a–d shows typical relation between molar magnetic susceptibility (χ_M) and absolute temperature as a function of the magnetic field intensities (833, 1,280, 1,733, 2,160 Oe). From the figure, it is clear that the normal behavior of (χ_M) with temperature is the normal trend of ferrimagnetic spinel ferrites. In other words, at low temperature (ferrimagnetic), the thermal energy which affects on the sample is not enough to overcome the impact of the magnetic field which aligns the spins in its direction. The result is the slow decrease of (χ_M) with increasing temperature. While, in the high temperature region (paramagnetic), the thermal energy increases the lattice vibration as well as the disordered state of spins causing the rapid decrease in (χ_M).

The variation of Curie temperature T_C with Ag content (x) was observed in Fig. 5a. Introducing Ag^{1+} ions with large ionic radius (1.26 Å) increases the ratio of Fe^{2+}/Fe^{3+} on the B sites, after that, some of Fe^{2+} ions could migrate from B to A sites which decreases directly the net magnetization of the system. Variation in the oxygen content due to the difference between the valances of Fe^{3+} and Ag^{1+} can affect the interaction distance and angle that lead to a change in the magnetic interaction [24]. In other words, the exchange interactions between the magnetic ions on A and B sublattices increase with both the density and the magnetic moment of the magnetic ions. Greater amount of thermal energy is required to offset the effects of exchange interactions. The increase of Ag^{1+} ions' content after $x = 0.2$, decreases the number of iron (Fe^{3+}) ions available on B sites. Consequently, a redistribution of the metal cations takes place in the spinel matrix resulting in an increase in T_C.

The values of the effective magnetic moment μ_{eff} at different Ag content (x) as a function of magnetic field intensity are shown in Fig. 5b. It is clear that, slight decrease in the effective magnetic moment with increasing Ag^{1+} content. The replacement of Mg^{2+} from A to B sites at the expense of Fe^{3+} which go to A sites as Fe^{2+} has larger ionic radius causes disruption of the magnetic ordering of Mg^{2+} and Fe^{3+} ions leading to decrease of μ_{eff} as mentioned before.

Electrical conductivity and thermoelectric power

Room temperature dc resistivity (ρ_{dc}) of all prepared samples was measured as a function of Ag content (x) as seen in Fig. 6. The data show that, the conductivity increases with

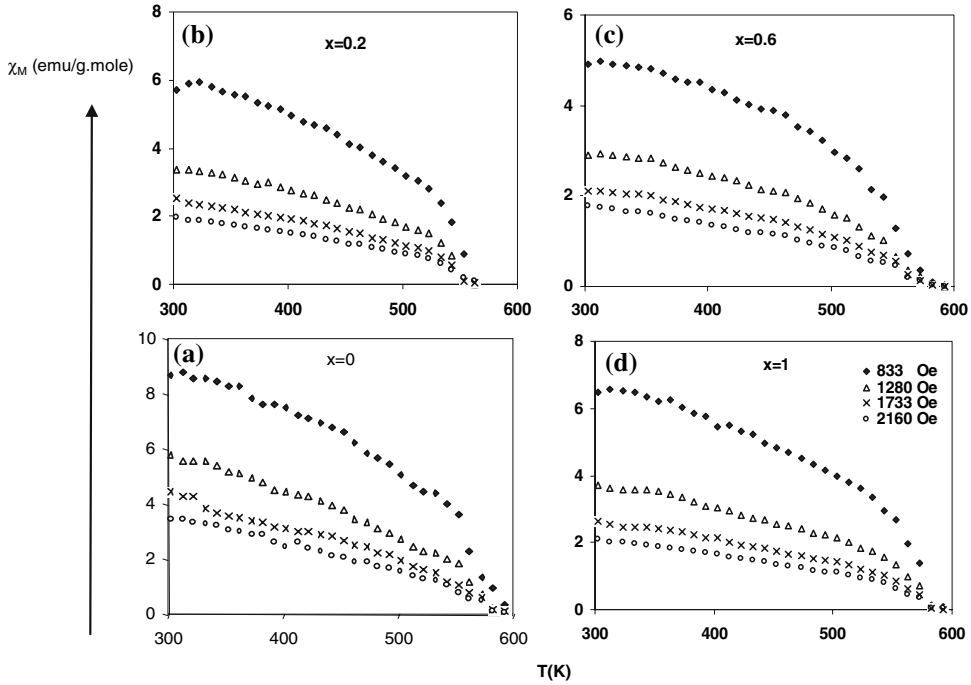

Fig. 4 Temperature dependence of the dc molar magnetic susceptibility for the investigated samples as a function of magnetic field intensity

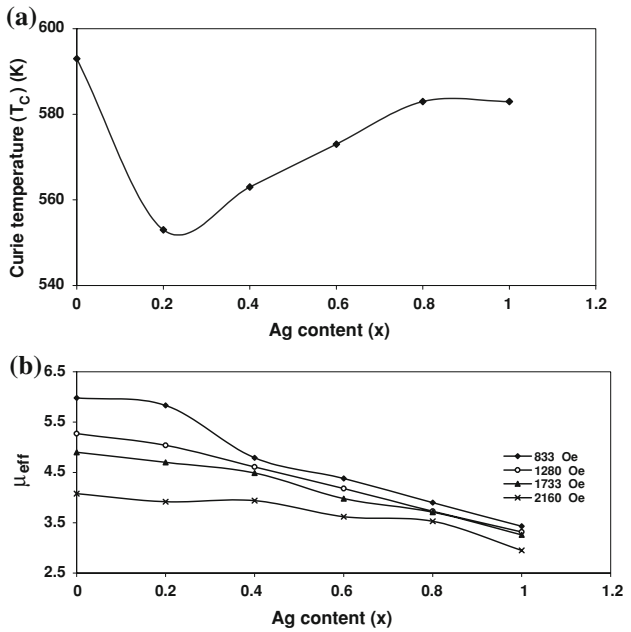

Fig. 5 (**a**) The values of Curie temperature (T_C) as a function of Ag content (x). (**b**) Dependence of the effective magnetic moment (μ_{eff}) on Ag content (x)

Ag content. This increase in the conductivity may be due to the reason that Ag^{1+} ions has less resistivity ($\rho = 1.62$ Ωcm) than Mg ($\rho = 4.46$ Ωcm). On increasing Ag^{1+} ion substitution, the number of ferric and ferrous ions on B sites increases. Consequently, the conductivity increases.

The variation of *Seebeck* coefficient (S) with average absolute temperature is shown in Fig. 7. The figure shows

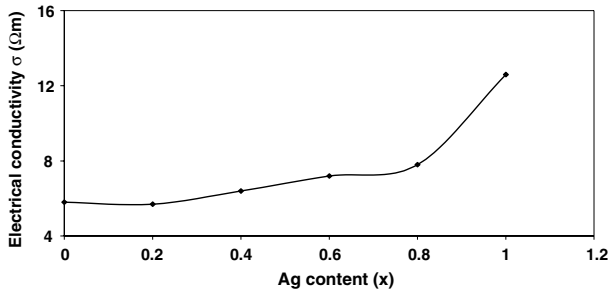

Fig. 6 Variation of dc conductivity (σ_{dc}) with Ag content (x)

that, the trend of (S) for all Ag contents (x) is positive (p-type) except $x = 0$, Mg ferrite is n-type [25]. Moreover, all the samples show an increasing trend in S with temperature. The temperature of maximum S is roughly correlated to the Curie temperature. The magnetic ordering has an influence on S. Therefore, an increase in S with increasing Ag has an effect on reducing the number of Fe^{2+} ions on B sites. Overall, the conduction mechanism (p-type) can be explained on the basis of migration of some Fe^{3+} ions from B to A sites. This migration might result in the formation of excess vacancies. A similar variation of (S) with temperature was observed in Mg–Ga [26] and Cu–Zn [27] ferrite.

Conclusions

The flash combustion technique gives better microstructure and chemical homogeneity. Also, this method is simple and does not require elaborate instrumental set-up. The ferrite

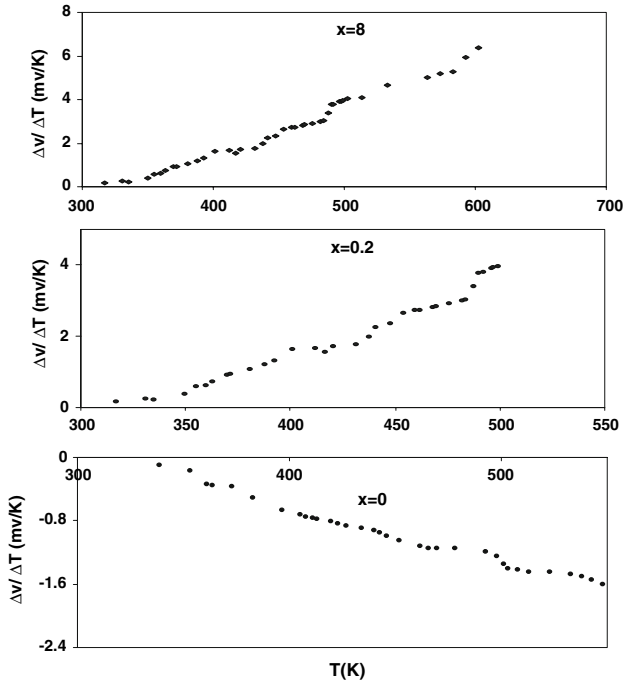

Fig. 7 Variation of *Seebeck* coefficient (*S*) with absolute temperature (T_K)

materials prepared by this method are pure, highly reactive, because of the atomic level mixing of the starting materials and this gives good magnetic and electrical properties. The presence of silver ions in the investigated ferrite improves the electrical conductivity and Curie temperature. The positive sign of thermoelectric power (p-type) increases with increasing Ag^{1+}. Due to high electrical conductivity of silver metal ions, it can be used as an electrode material as applicable.

References

1. Ahmed MA, El-Khawas EH, Hassan MY, El-Desoky M (2000) Indian J Phys 74A(6):451
2. Ahmed MA, Ateia E, El-Dek SI (2002) J Vib Spectrosc 30:69
3. Amer MA (2000) Phys Status Solidi A 181:539
4. Goldman A (1990) Modern ferrite technology. Van Nostrand, New York
5. Augustin CO, Prabhakaran D, Srinivasan LK (1993) J Mater Sci Lett 12:383
6. McMillan JA (1960) J Inorg Nucl Chem 13:28
7. Scatturin V, Bellom P, Salkind AJ (1960) Ric Sci 30:1034
8. Reiding AB, Kazarnovski IAK (1951) Dokl Akad Nauk SSSR 78:713
9. Schwab GM, Hartmann G (1955) Z Anorg Allg Chem 281:183
10. Mckie AS, Clark AD (1963) Batteries, vol 285. Pergamon, Oxford
11. Behera D, Nishra ND, Patnaik K (1997) J Supercond 10:27
12. Sperka G, Fritzer HP (1988) J Solid State Commun 65:1275
13. Song K-H, Dou S-X, Sorrell CC (1991) J Phys C 185:2387
14. Prout EG, Thompkins FC (1946) Trans Faraday Soc 42:468
15. Prout EG, Sole MJ (1959) J Inorg Nucl Chem 9:232
16. Boonstra G (1968) Acta Cryst B 24:1053
17. Chang FM, Jansen M (1984) Krist Z 169:295
18. Balagopal N, Warrier KGK, Damodaran AD (1991) J Mater Sci Lett 10:1116
19. Assal J, Hallstedt B, Gauckler LJ (1997) J Am Ceram Soc 80:3054
20. Verwey EJ, Heilman EL (1947) J Chem Phys 15:174
21. Kulkarni R, Joshi H (1985) Solid State Commun 53:1005
22. Mazen SA, Abdallah MH, Sabrah BA, Hashem HAM (1992) Phys Status Solidi A 134:263
23. Wang S-F, Wang Y-R, Yang TCK, Wang P-O, Lu C-A (2000) J Mag Mag Mater 217:35
24. Dogra A, Kumar R, Khan SA, Sivakumar VV, Singh M (2004) Nucl Instrum Meth Phys B 225:283
25. Shaikh AM, Kanamadi CM, Chougule BK (2005) J Mater Chem Phys 215:103
26. Abdel Malik Md, Reddy VD, Venugopal Reddy P, Sagar DR, Prankishan (1994) J Mod Phys Letts 16:947
27. Ravinder D (1999) J Alloys Comps 291:208